

Multi-angle Oblique Optical Coherence Tomography

Mikael Malmström
tf05mm1@student.lth.se

August 28, 2008

Abstract

Optical Coherence Tomography (OCT) is a non-invasive high-resolution method for measuring the reflectance of scattering media in 1/2/3D, e.g. skin. The method has been used in a number of different medical fields and for measurement of tissue optical properties.

The software developed in this thesis is able to display features hidden in a shadowed volume by adding multiple OCT measurements taken at oblique angles, a technique here called Multiple-Angle Oblique Optical Coherence Tomography (MAO-OCT).

Three different objects with were measured at 5 to 9 angles. The measurements were automatically and manually aligned in the software. They were also tested with 6 different high pass intensity filters (HPIF) and reduced in size using 4 different methods to speed up calculations.

The software's automatic alignment was tested with one tilted computer generated test at 9 angles and with 5 different shadow strengths.

With MAO-OCT it is possible to remove some effects of shadows in OCT, though it comes with a cost of reduced sharpness. The errors depend much on the differences in index of refraction in the sample.

The software managed to automatically align 90% of the artificial measurements, and 60% of the OCT measurements. The shadow strength and the resize method had no noticeable effect on the automatic alignment of the measurements.

List of Abbreviations

CT	Computed Tomography
DICOM	Digital Imaging and Communications in Medicine
GUI	Graphical user interface
HPIF	High pass intensity filter
MRI	Magnetic Resonance Imaging
ROI	Region of interest
SNR	signal-to-noise ratio, for signals $SNR = \frac{P_{signal}}{P_{noise}}$ and the ratio of the mean pixel value to the standard deviation of the pixel values.
MAO-OCT	Multi-angle Oblique-OCT
OCT	Optical Coherence Tomography
SS-OCT	Swept Source-OCT

Contents

List of Abbreviations	i
1 Introduction	1
1.1 Background	1
1.2 State of research	3
1.3 Problem description and motivation for MAO-OCT	3
2 Physical and technical principles of the applied methods	6
2.1 Optical Coherence Tomography	6
2.2 Definitions	8
2.3 The Matlab GUI "OCT Combine"	10
2.3.1 Rotation of slices	10
2.3.2 Finding offset	12
2.3.3 Finding rotation/tilt and offset with golden section search	12
2.3.4 Master transformation	13
2.3.5 Automatic alignment, (I'm feeling lucky)	13
2.3.6 Rescaling of measurements	13
2.4 3D volume rendering in OsiriX	14
3 Experimental setup and methods	16
3.1 Setup	16
3.1.1 The OCT system	16
3.1.2 Matlab GUI	17
3.2 Methods	17
3.2.1 Evaluation of MAO-OCT	17
3.2.2 Evaluation of OCT Combine GUI	18
4 Results	20
4.1 Evaluation of MAO-OCT	20
4.2 Evaluation of OCT Combine GUI	24

4.2.1	Automatic aligning and sensitivity of shadows	24
4.2.2	Automatic aligning of MAO-OCT measurements	25
5	Discussion	29
5.1	Evaluation of MAO-OCT	29
5.1.1	Index of refraction	29
5.1.2	Reflections	29
5.2	Automatic aligning capability	31
5.2.1	Shadow strength	31
5.2.2	Saving method	31
5.2.3	HPIF threshold	32
5.2.4	Resizing method	32
5.2.5	Other aspects affecting the alignment	32
6	Conclusions and future work	35
6.1	New measurements	35
6.2	Combining improvements	35
6.3	Aligning improvements	36
6.4	Future work	36
	Bibliography	37
	A Getting started with OCT Combine	39
	B OCT Combine flowchart	42

Chapter 1

Introduction

The author is following the Master of Science in Engineering Physics program at the Faculty of Engineering at Lund University (LTH). He has focused his studies on lasers and optics. The master thesis was done under the supervision of Dr Jan Dam at the National Laser Center (NLC) of the Council for Scientific and Industrial Research (CSIR) in South Africa, and Professor Stefan Andersson-Engels at the Medical Laser Physics Group of the Atomic Physics Division, LTH.

CSIR is one of the leading scientific and technology research, development and implementation organizations in Africa. It undertakes directed research and development for socio-economic growth.

The biophotonics research group, led by Dr Jan Dam, consists of five researchers with a comprehensive background in the fields of physics, microbiology, biomedical optics, and biochemistry. The activities of the group are primarily aimed at the development and improvement of various therapeutic and diagnostic medical applications of lasers. These applications include low level laser therapy for wound healing and photodynamic therapy for non-invasive cancer treatment.

1.1 Background

There is a variety of different non, or minimally-invasive methods for imaging in vivo today for example Magnetic Resonance Imaging (MRI), Computed Tomography (CT) and ultrasound. These methods rely on different physical processes in order to achieve the imaging. MRI uses an RF-signal to assess the amount of hydrogen in an area by looking at the resonance signal from the hyperfine structure in hydrogen. CT uses X-ray scans from various angles around the object and the signal is dependent on density and chemical

composition along the path. Ultrasound uses sound waves and measures the reflected signal, which is affected by absorption and differences in acoustical impedance in the body. The image reconstruction for the different modalities is then performed with various algorithms.

Differences in penetration depth, resolution, noise, acquisition time, cost and physical harm make the above-mentioned imaging modalities useful in different areas. This thesis studies another method, Optical Coherence Tomography (OCT).

OCT works similar to ultrasound but uses light instead of sound. The reflected signal can be used to create volume images of the reflectance in the studied object, for example skin.

Tissue is a highly scattering and absorbing media, so one has to choose a suitable wavelength in order to penetrate and get a sufficient signal back from the tissue. Figure 1.1 shows the absorption of light as a function of wavelength for the different chromophores in tissue. One can see that the so-called *tissue optical window* is situated in the near infrared region from around 630 nm up to about 1300 nm [9, 11]

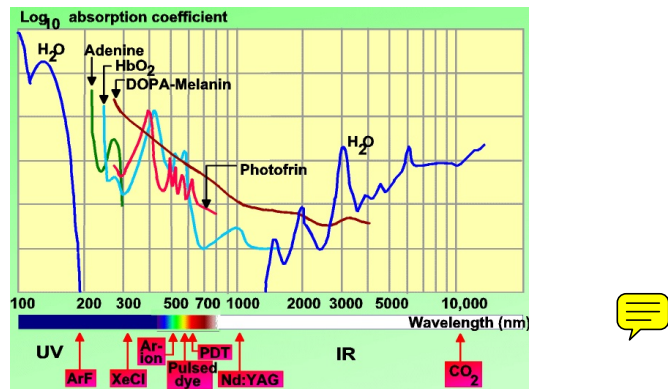


Figure 1.1: Absorption spectra of tissue chromophores.

Because of the high scattering in skin the penetration depth of an OCT-system is only in the order of mm, on the other hand the resolution is in the order of 4-16 μm [4] (for this system it is 9-15 μm [12]). This is compared with the most MRI systems having a resolution above 500 μm , CT have a resolution in the order of mm and the best high-frequency ultrasound system have a resolution of about 80-90 μm . At the moment the only cross sectional method with better resolution than OCT is confocal microscopy, unfortunately its penetration depth is typically in the range of 100 μm [3].

1.2 State of research

OCT has been used as a non-invasive high resolution imaging method in a number of different medical fields [2, 8, 13]. It has also been proposed and used for measurements of tissue optical properties [5, 10].

1.3 Problem description and motivation for MAO-OCT

As opposed to the conventional way of acquiring single 3D images with an OCT system, described more in detail later, the technique proposed here, Multi-angle Oblique OCT (MAO-OCT) is based on several volume-scans performed at an oblique angle. The different measurements are put together to form a single 3D volume, see Figure 1.2.

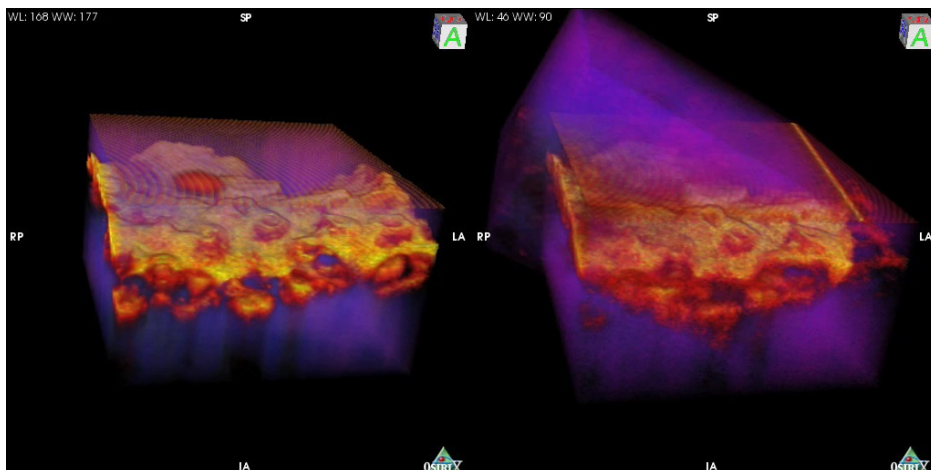


Figure 1.2: Principle of Multi-angle Oblique-OCT. To the left is a conventional OCT 3D image and to the right is two measurements added together.

The main reason for investigating MAO-OCT is that such technique could reveal information about deep positioned objects that might be shadowed by highly scattering objects above it, see Figure 1.3. Looking at the oblique measurements one by one could also reveal that information but the aim here is to get the whole picture at once.

Another motivation is that adding several measurements together should increase signal-to-noise ratio (SNR) as the square root N where N is the independent number of measurements. This is due to the nature of the speckle obeying Gaussian statistics [10]

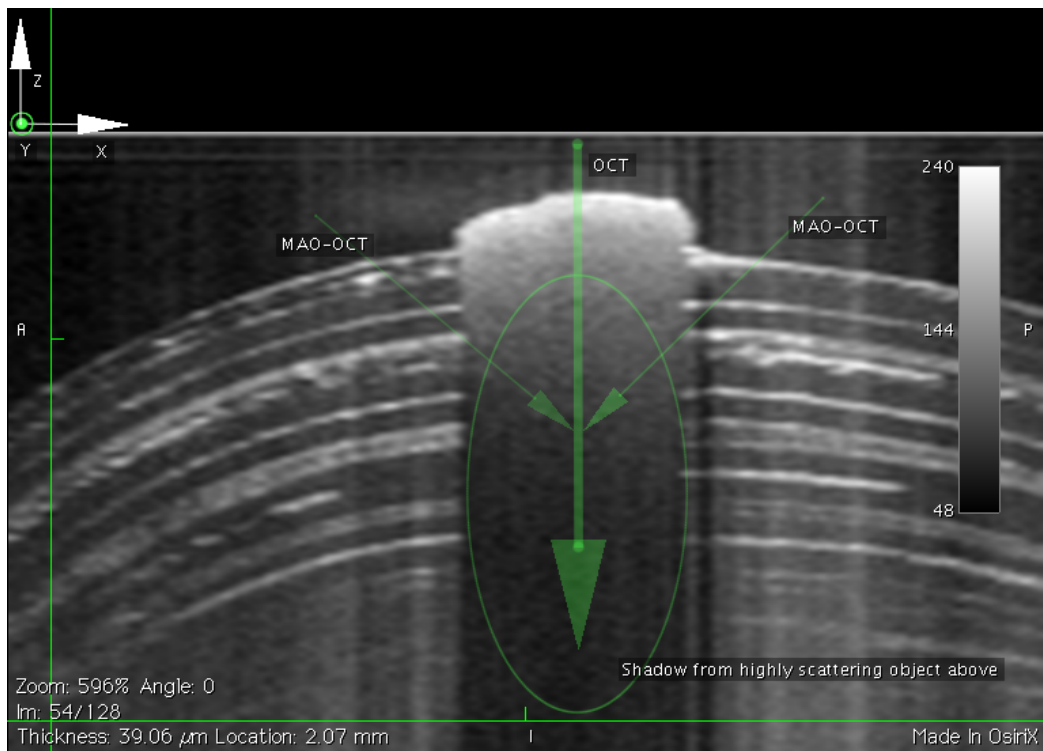


Figure 1.3: Conventional B-scan and proposed MAO-OCT geometry to see hidden object.

It is the goal of this thesis to develop a tool for adding MAO-OCT measurements together and evaluate the use as well as the performance of this tool.

Chapter 2

Physical and technical principles of the applied methods

2.1 Optical Coherence Tomography

OCT is based on low coherence interferometry and uses light as oppose to the other technics mentioned in the introduction (except confocal microscopy). Basically the OCT works like modified Michelson interferometer. A low coherence light beam is divided by a 50/50 beam splitter. One half of the beam goes straight through the beam splitter into the reference arm. This beam travels a known distance to a mirror which reflects the beam back to the beam splitter where half of it is directed onto a detector, see Figure 2.1, this distance is called z_r . The second half of the original beam is directed by the beam splitter into the sample where it is partly reflected at various depths in the sample. Some of this reflected light travels back through the beam splitter and hits the same detector, this part of the beam will have traveled the distance z_s . Since both beams have the same origin, the two will interfere and create an interference pattern at the detector.

The interference pattern will depend on both the reflected amount of light and the depth from where it was reflected in the sample, i.e. the difference between z_r and z_s . Light outside of the coherence length will not interfere significantly. In a conventional OCT system the reference mirror is moved causing the distance z_r to change creating a fairly complicated pattern on the detector. From this a plot of the reflectance as a function of depth (i.e. -Z in Figure 2.2) can be reconstructed, a so-called A-scan. A B-scan is acquired when a series of A-scans are taken along a direction (i.e. X in Figure 2.2) and put together to form an image. Subsequently the 3D-volume image can be completed by taking a series of B-scans along another direction (i.e. Y in

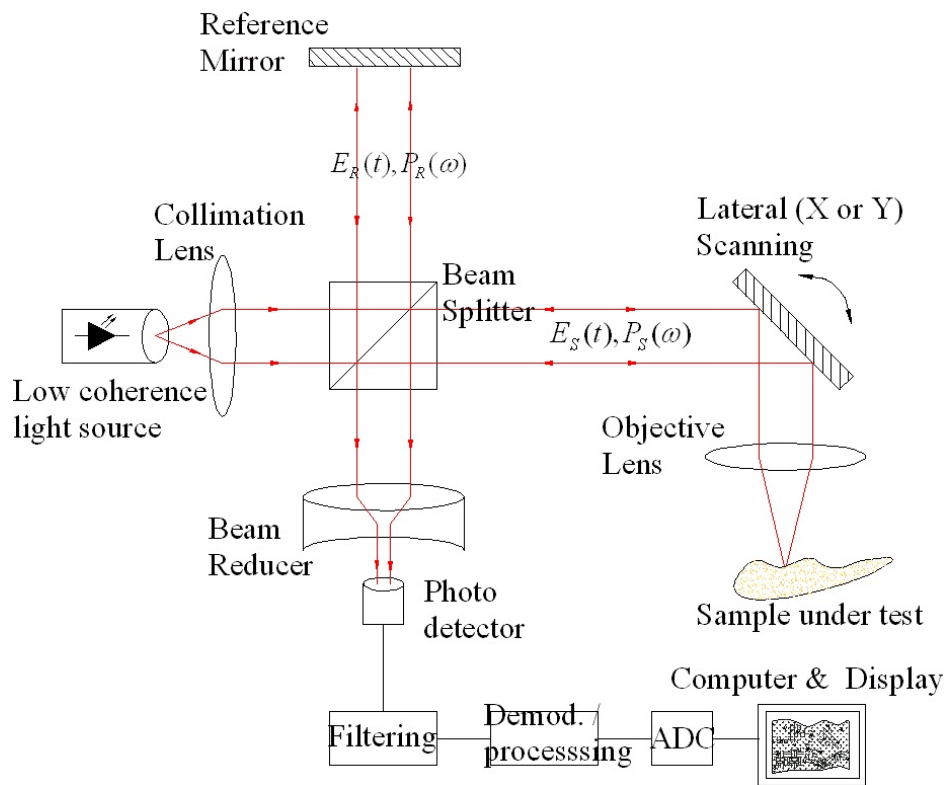


Figure 2.1: OCT B-scan recording (courtesy of User:Pumpkinegan [15], image is modified under the Creative Commons Attribution-ShareAlike 2.5 License)

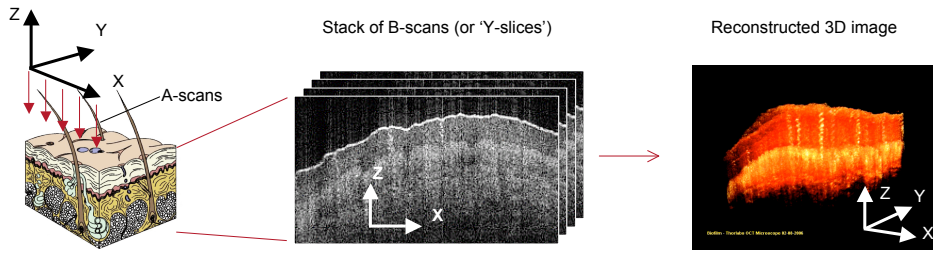


Figure 2.2: OCT recording and subsequent volume imaging

Figure 2.2)

For a more detailed explanation and the mathematics behind the extraction of information please refer to [2, 3, 7].

2.2 Definitions

1. There are some different coordinate systems used by the different softwares, but they are all right hand systems. See Figure 2.3
 - (a) The first one XYZ-system is used by the OCT system representing voxels and is indexed by integers. The $-Z$ -direction is in the direction of the beam. Origo is in the upper left corner of the sample. The system starts with scanning A-scans along the X-axis resulting in a B-scan, then progressing along the Y-axis.
 - (b) When imported to Matlab the matrix described by [row column depth] equals the $[-Z X Y]$ dimensions of the OCT system (note depth in the matrix is the third dimension not the vertical depth in the sample i.e. Y not $-Z$).
 - (c) OsiriX, the software used for rendering 3D images, uses the same system as the OCT system but also denotes each side. The measurement is labeled with left and right as if it was looking in the negative Y direction (see Figure 2.3), it also has a front called anterior and a back called posterior as well as superior for the top and inferior for the bottom.
2. A **Slice** is the plane perpendicular to an axis, it can be taken at any point along the axis. Here the Z-slice (XY-plane) is represented by the color green, X-slice (YZ-plane) by red and Y-slice (ZY-plane) by blue, see Figure 2.4. For example in Matlab the Y-slice of a measurement \mathbf{A} can be represented by $\mathbf{A}(1:\text{end}, 1:\text{end}, i)$ where i is an integer specifying where on the Y-axis, the slice is taken.

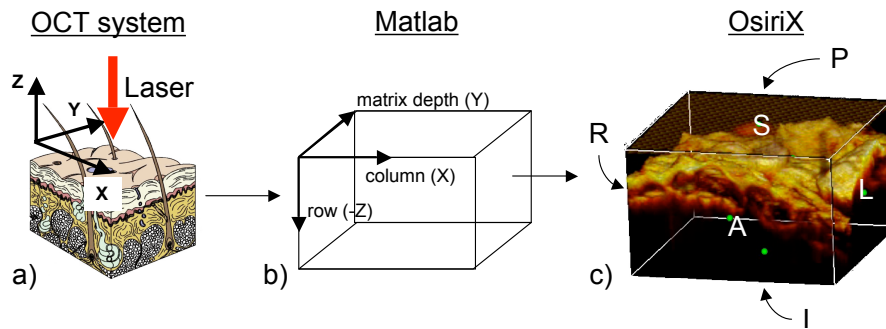


Figure 2.3: a) Coordinate system used by the OCT system, b) corresponding matrix coordinates in Matlab c) corresponding coordinate system in OsiriX (the letters means for Left, Right, Anterior Posterior, Superior and Inferior).

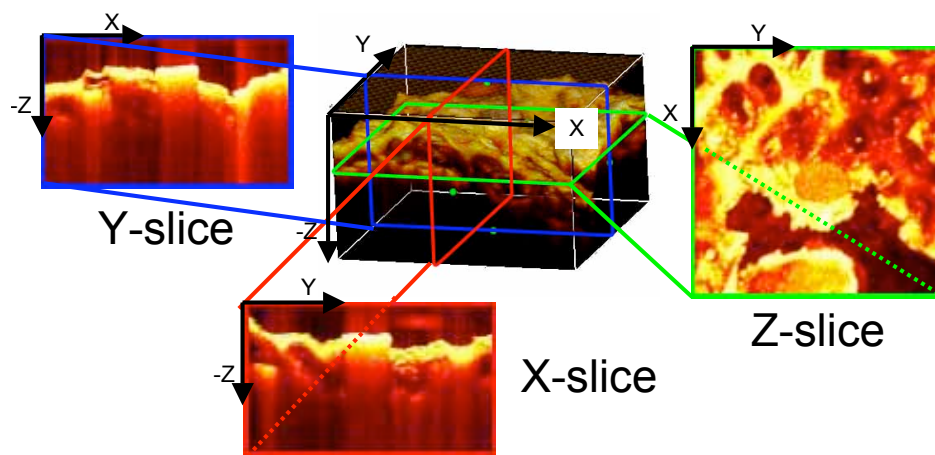


Figure 2.4: The Z, X and Y coordinate system of the OCT system, and the orientation of the different slices. The measured object is a piece of mandarin peel. The Z-slice is represented by green, X-slice by red and the Y-slice is represented by blue.

3. **Rotation** of a measurement is the right hand rotation around the Z-axis, the center of rotation is the center of the measurement. A positive rotation of a slice/image is the CCW rotation around its center.
4. **Tilt** of a measurement is the right hand rotation around the X or Y-axis with center of measurement as center of rotation.
5. The **Region of interest** (ROI) is generally a 2D or 3D region of special interest. For "OCT Combine", a "graphical user interface" (GUI) described later, it is a point in the sample at the center of the region of special interest. The slices displayed in OCT Combine all go through this point.

2.3 The Matlab GUI "OCT Combine"

The general purpose of the GUI is to align and stitch two measurements of the same object with different observation angle. In order to align two 3D measurements with a 2D screen the Z, X and Y-slices taken at the position of the ROI are displayed and compared. By moving the ROI one can compare the alignment at different places in the measurements.

OCT Combine, shown in Figure 2.5, can be run manually to find the rotation and offset between the measurements, but it has also been developed in order to automatically find the alignment of two or more measurements.

A flowchart for the different functions and sub functions used can be found in Appendix B, and some of the more important functions will be described below.

2.3.1 Rotation of slices

In order to align different MAO-OCT measurements one of them have to be rotated and tilted. The measurements produced by the OCT system can have various dimensions in the different directions. A rigid rotation of an image does not take the pixel spacing in to account so in order to rotate such an image properly an affine transformation has to be performed, see the difference in Figure 2.6.

The new area outside the rotated measurement is padded with zeros, the black area in the rotated 2nd measurement in Figure 2.6.

From now on the rotation/tilt of a slice, sample or measurement will imply the affine transformation taking the pixel spacing in to account.

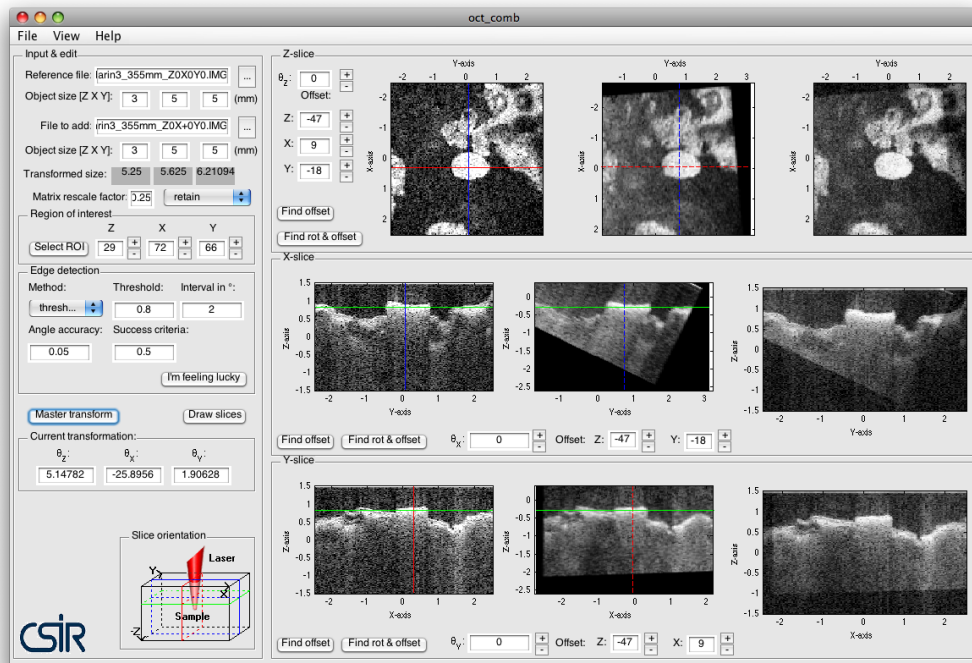


Figure 2.5: Screen shot of the developed software oct_comb while aligning two measurements.

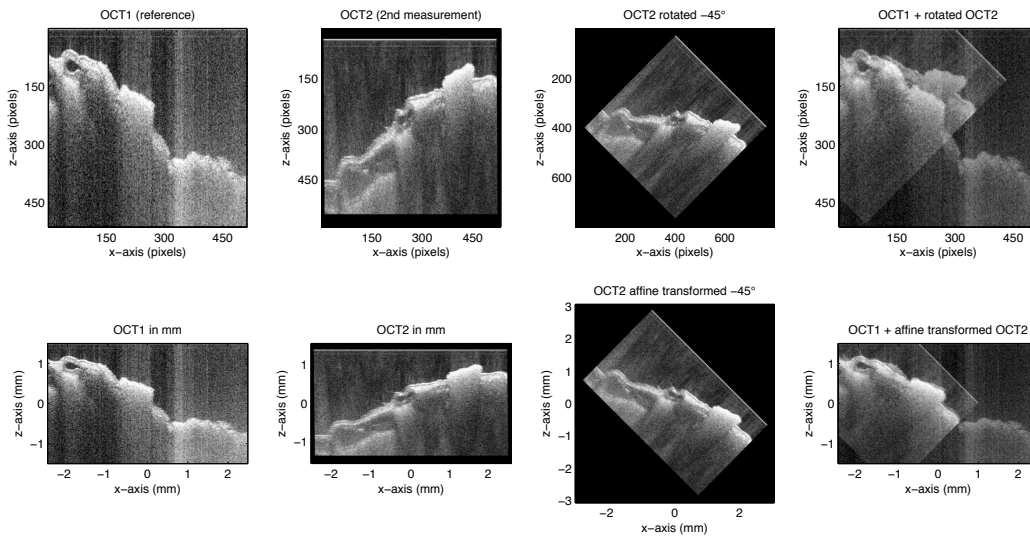


Figure 2.6: The difference between rotation and affine transformation when measurement has different pixel spacing in the horizontal and vertical direction. Top row, illustration of rotation and bottom row, affine transformation.

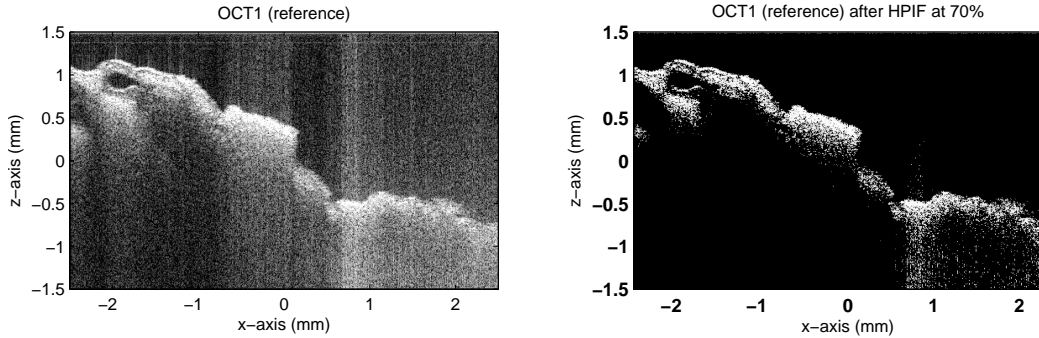


Figure 2.7: To the left is the original image and to the right is the HPIF filtered image where only the prominent features are left

2.3.2 Finding offset

The function for finding the offset between two images relies on a 2D cross correlation between the two. Before the images are correlated they are filtered with a high pass intensity filter (HPIF), stripping them of their pixels below a certain threshold, i.e. removing the lower part of the image histogram, see Figure 2.7. The HPIF increases processing speed of the cross correlation and reduces the risk of miss fitting the images due to speckles. The offset is then given by the position of the maximum value in the cross correlation matrix.

2.3.3 Finding rotation/tilt and offset with golden section search

By putting together the two functions for rotating slices and finding offset described above, in a golden section search [6, 14] the rotation/tilt and offset between two images can be found at the same time. A golden section search locates a unimodal function's extremum on a specified interval. It is achieved by probing the function at certain points separated by the golden ratio, then narrowing the interval depending on the function value at the points.

The function used here is the maximum value of the cross correlation matrix as a function of the rotation of the second image. It is assumed that the function will have a maximum when the images are aligned. The algorithm keeps narrowing the angle interval until the change is less than a specified value.

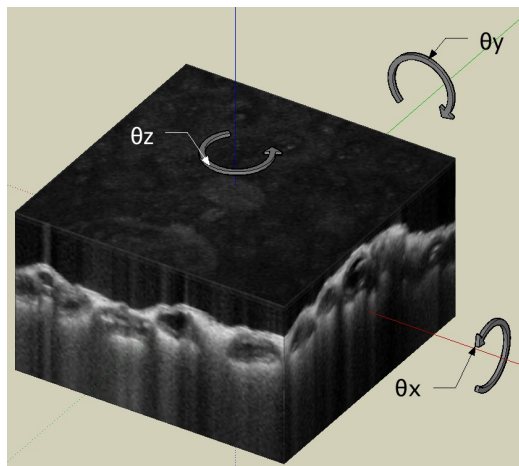


Figure 2.8: The orientation of the rotation axes

2.3.4 Master transformation

After finding the best fit regarding tilt and rotation between the reference measurement and the second measurement a so-called master transformation is performed on the latter. Here all the slices along one axis at a time are rotated starting with the Z-axis followed by the X- and last the Y-axis resulting in a rotated and tilted 3D-volume, see Figure 2.8.

2.3.5 Automatic alignment, (I'm feeling lucky)

OCT Combine has been equipped with a automatic alignment tool. The button, called "I'm feeling lucky" utilizes a series of golden section searches and master transformations in order to align the measurements together. First a rough alignment is performed with a wide interval of $\pm 5^\circ$ and a low accuracy, then a finer adjustment performed. If the angle between the measurements is bigger than the interval the found angle will most likely be close to the edge of the interval. Then the interval moved and the search is repeated.

2.3.6 Rescaling of measurements

A typical OCT measurement is $512 \times 512 \times 512$ voxels of 8-bit grayscale. Working with two measurements in the memory and doing cross correlations of their slices requires a computer preferably faster than a 2x2GHz Intel Core duo in order for calculation times to be manageable. Additionally it requires more than 2 GB RAM in order to run properly.

In order to reduce the computation times it is possible to down size the measurements to more reasonable size. The size 128x128x128 is 1/32 of the typical measurement and decreases the computation times by about the same. When the rotation and tilt have been found the user can choose to go back to the original size for some last rotation and offset adjustments.

Four different methods of down scaling are used here called, retain, nearest, bilinear and bicubic. For example when rescaling a 512x512x512 measurement to 128x128x128 (a factor 0.25 in every direction) the methods works like follows:

retain is based on Matlabs function `reducevolume` and retains every 4th (1/0.25) element in every dimension.

nearest is based on multiple usage of function `imresize` uses nearest neighbor interpolation (here about 160 times slower than retain).

bilinear is based on multiple usage of function `imresize` uses bilinear interpolation (here about 1000 times slower than retain).

bicubic is based on multiple usage of function `imresize` uses bicubic interpolation (here about 1200 times slower than retain).

Figure 2.9 shows the result for the different resizing methods.

2.4 3D volume rendering in OsiriX

When the measurements are aligned they can be combined and exported to Digital Imaging and Communications in Medicine (DICOM) format which can be imported by OsiriX. OsiriX is an open-source software developed for 2, 3 and 4D imaging of medical applications, see Figure 2.10. It handles images produced by a number of different modalities such as MRI, CT ultrasound and many more (see PS 3.16 "Content Item Descriptions (CID) 29 Acquisition Modality" in [1]).

The aligned and combined measurements are exported with a here-developed function called `OCT_series2DICOM` that pass on the pixel spacing and orientation of the slices. When the measurements are imported in OsiriX, they can be compared with the reference in 2D and 3D.

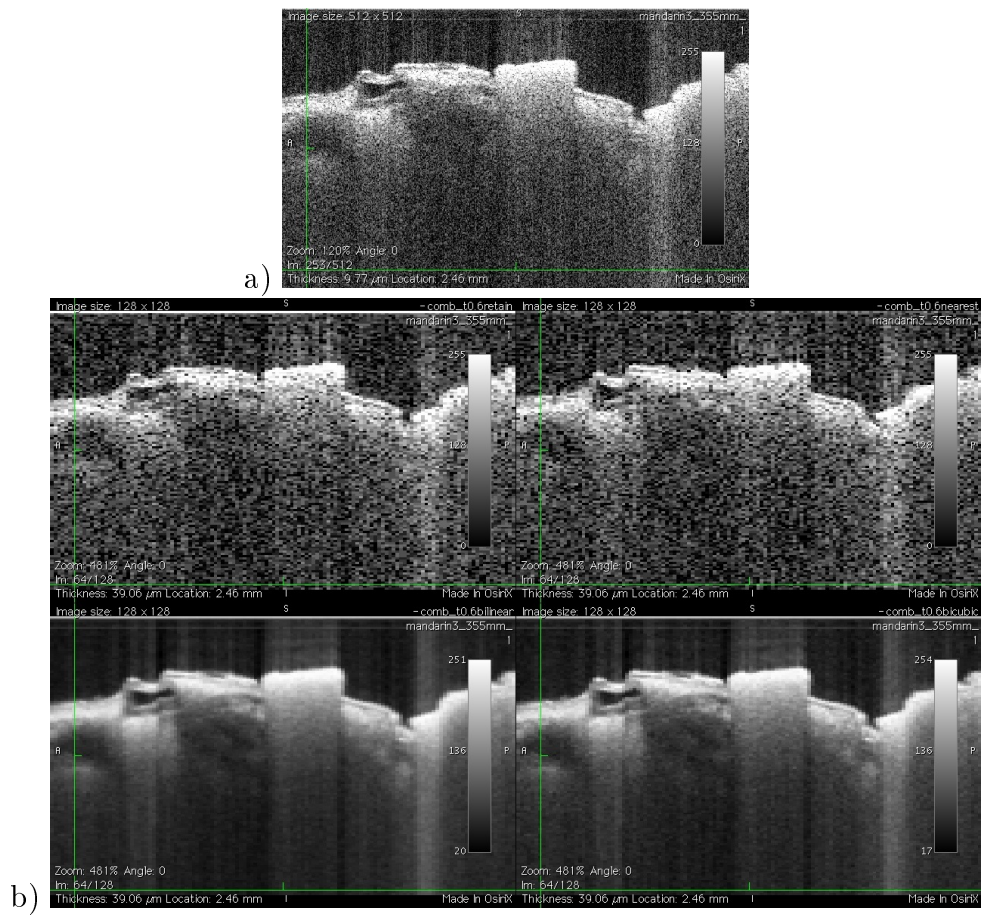


Figure 2.9: a) Y-slice from the reference measurement of a mandarin peel. b) Four corresponding Y-slices from the same measurement but processed with four different rescaling methods. Top left used retain and right nearest, bottom left used bilinear and for the right one bicubic rescaling was used

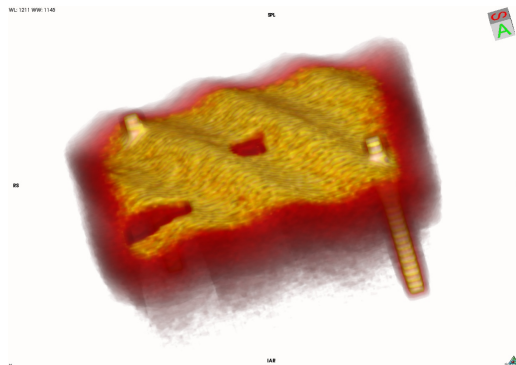


Figure 2.10: An image from OsiriX of a computer generated "test chunk".

Chapter 3

Experimental setup and methods

3.1 Setup

3.1.1 The OCT system

The measurements in this thesis are made with a Thorlabs' OCM1300SS OCT system shown in Figure 3.1. The system works similar to the conventional OCT system described in section 2.1 but OCM1300SS utilizes fibers and a swept source (SS-OCT) instead of a moving mirror and has a central wavelength at 1325 nm. Since there are no moving parts high axial scanning rates can be achieved [2].

A schematic picture of how the OCT system operates is shown in Figure 3.2



Figure 3.1: Thorlabs' OCM1300SS OCT system

The system is able to save the A-scans with 2048 data points in 16-bits but in this thesis a 8-bit grayscale and 512 to is used resulting in a 512x512x512 uint-8 matrix in Matlab. The matrix is reduced to 128x128x128

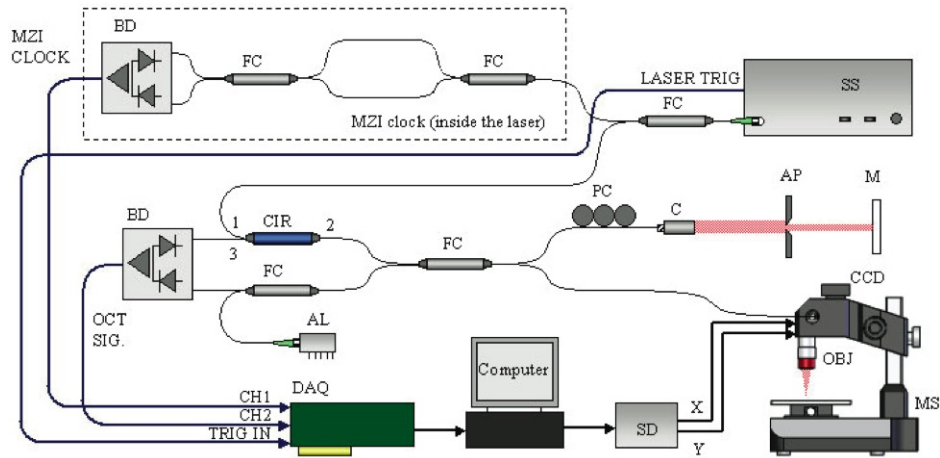


Figure 3.2: Schematic setup of the Thorlabs' OCM1300SS OCT system. (Note that the light travels in fibers instead of open air as in Figure 2.1)

for calculation speed.

For more info on the OCM1300SS please refer to [12]

3.1.2 Matlab GUI

The assembly of the OCT measurements were performed with OCT Combine which was developed and tested on a MacBook 2x2 GHz Intel Core duo with 2 GB RAM and a DELL Optiplex 745 with 3 GHz Intel Pentium D and 1 GB RAM.

3.2 Methods

3.2.1 Evaluation of MAO-OCT

In this part three objects, shown in Figure 3.3, were examined with the MAO-OCT technique at different tilt. A small piece of prestik (a rubber-like temporary adhesive) was put on the surface to get a shadowing effect shown in Figure 1.3.

The measurements were done over a $3 \times 5 \times 5$ mm volume at $512 \times 512 \times 512$ resolution. The objects were tilted back and forth around one of the X and Y-axis at a time resulting in 5 measurements including the reference measurement where the object was not tilted. The rigid character of the epoxy phantom allowed more controlled tilting so the object could also be tilted back and



Figure 3.3: The examined objects, from left to right, an old epoxy phantom made by my colleague Ann Singh used to simulate tissue optical properties, a dried piece of mandarin skin and a small roll of tightly packed paper and plastic.

fourth around the X and Y-axis simultaneously hence 9 measurements were obtained.

The three objects were aligned one by one with the aid of the automatic aligning but also fine tuned manually in order to get the best alignment. This alignment is referred to as the reference fitting.

3.2.2 Evaluation of OCT Combine GUI

Two tests were performed in order to evaluate the performance of the developed software. The first one tested the ability to assemble measurements depending on the strength of a shadow in the test object.

The second test evaluated the ability to automatically align the measurements of the objects in Figure 3.3 depending the threshold in the HPIF and the method of rescaling.

Automatic aligning and sensitivity of shadows

Several computer generated "test chunks" were created with various combinations of sine, cosine and exponential functions. The result was layered structure shown in Figure 3.4 with two vertical bars, a hole in one corner and a varied shadow in the middle.

These test chunks were tilted around the x and y-axes by an angle $0 \pm 14^\circ$ resulting in 9 artificial measurements of the same object. To simulate a highly reflective object laying on the top layer a shadow was created from a point on the top layer straight down in the tilted chunk. The shadow is visible as

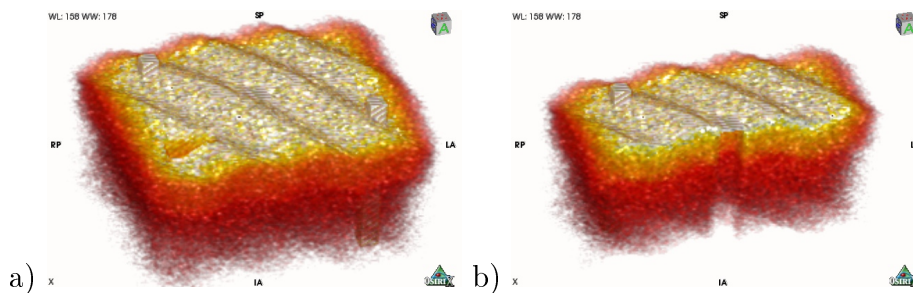


Figure 3.4: a) 3D image of test chunk. b) cropped chunk where the 100% shadow is visible as a hole in the chunk.

a hole in the middle of the 3D image in Figure 3.4. The shadow strength was varied by first creating the chunks then setting the intensity value of the voxels in the shadow region to 0, 20, ...100% of its original value. This way the automatic alignment could be tested in relation to the shadow strength.

Speckles were also added to the test chunks in order to simulate OCT measurements.

A script `eval_test_chunks.m` processed the files trying to automatically align each "measurement" with the reference measurement for each the different shadow strengths. The script was also run twice with two different modes of saving, `save_mat` and `save_add`.

`save_mat` aligns each measurement individually in the series with the reference measurement. If the software is able to find a fit, the two measurements are added together and saved in a new `.mat`-file. The difference with `save_add` is that the next file in the series is aligned not with the reference measurement alone but with the combination of the previously aligned measurements added together.

Automatic aligning of MAO-OCT measurements

A script `eval_mao.m` processed the files within three for loops, one for the different objects, one for the different HPIF thresholds and one for the different rescaling. It was also run twice with the two different modes of saving, `save_mat` and `save_add`

Chapter 4

Results

4.1 Evaluation of MAO-OCT

The three objects were aligned, stitched and imported to OsiriX. A few of the key slices showing the difference between the reference measurement and the aligned measurements are displayed in Figure 4.1, Figure 4.2 and Figure 4.3.

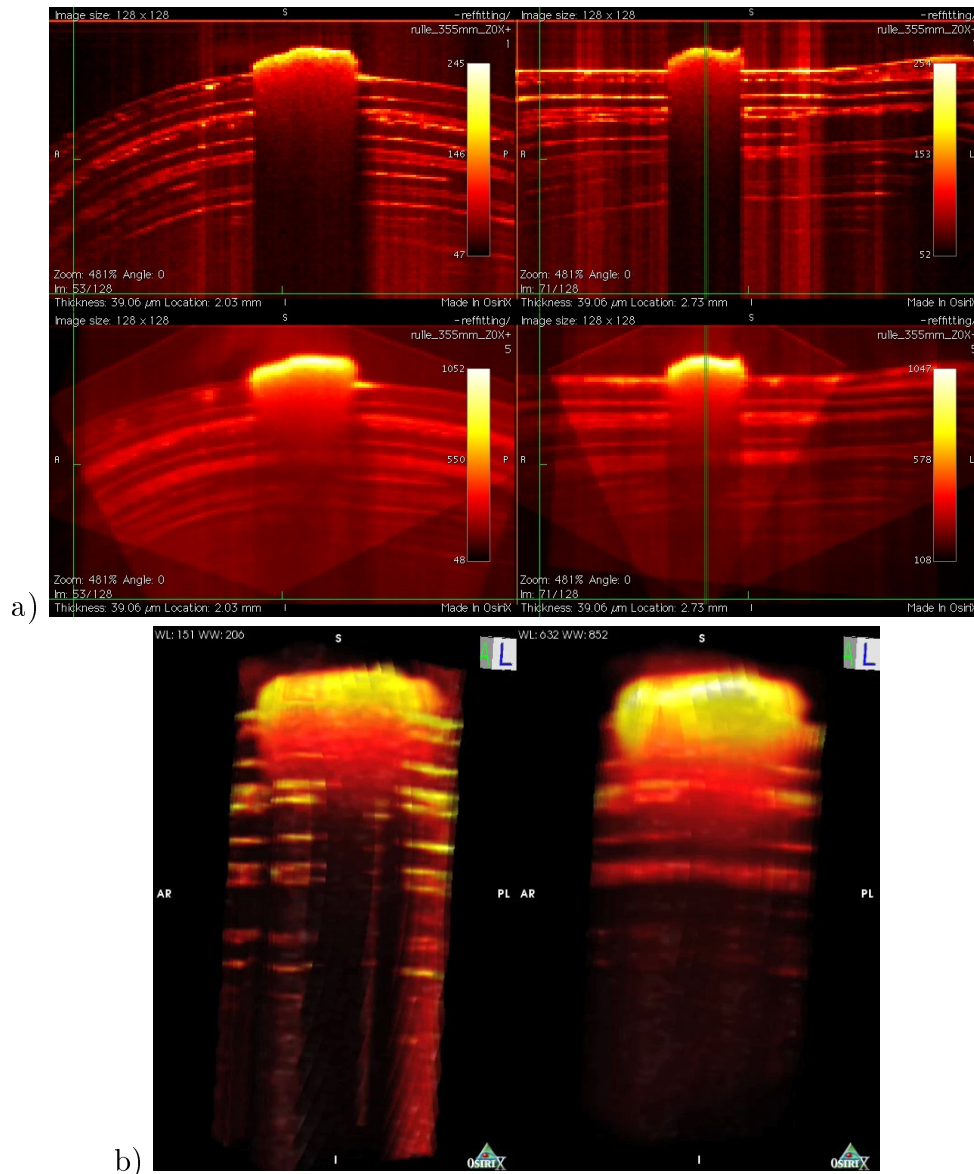


Figure 4.1: a) Top left, shows the reference measurement Y-slice with the shadow from the prestik visible in the middle, to the right is the X-slice of the same. The vertical green line in the X-slice shows where the Y-slice is located. The bottom row shows the same slice as above but with 4 added measurements. b) Shows a 3D image of the shadowed area under the prestik for the reference measurement to the left, and the combined measurement to the right.

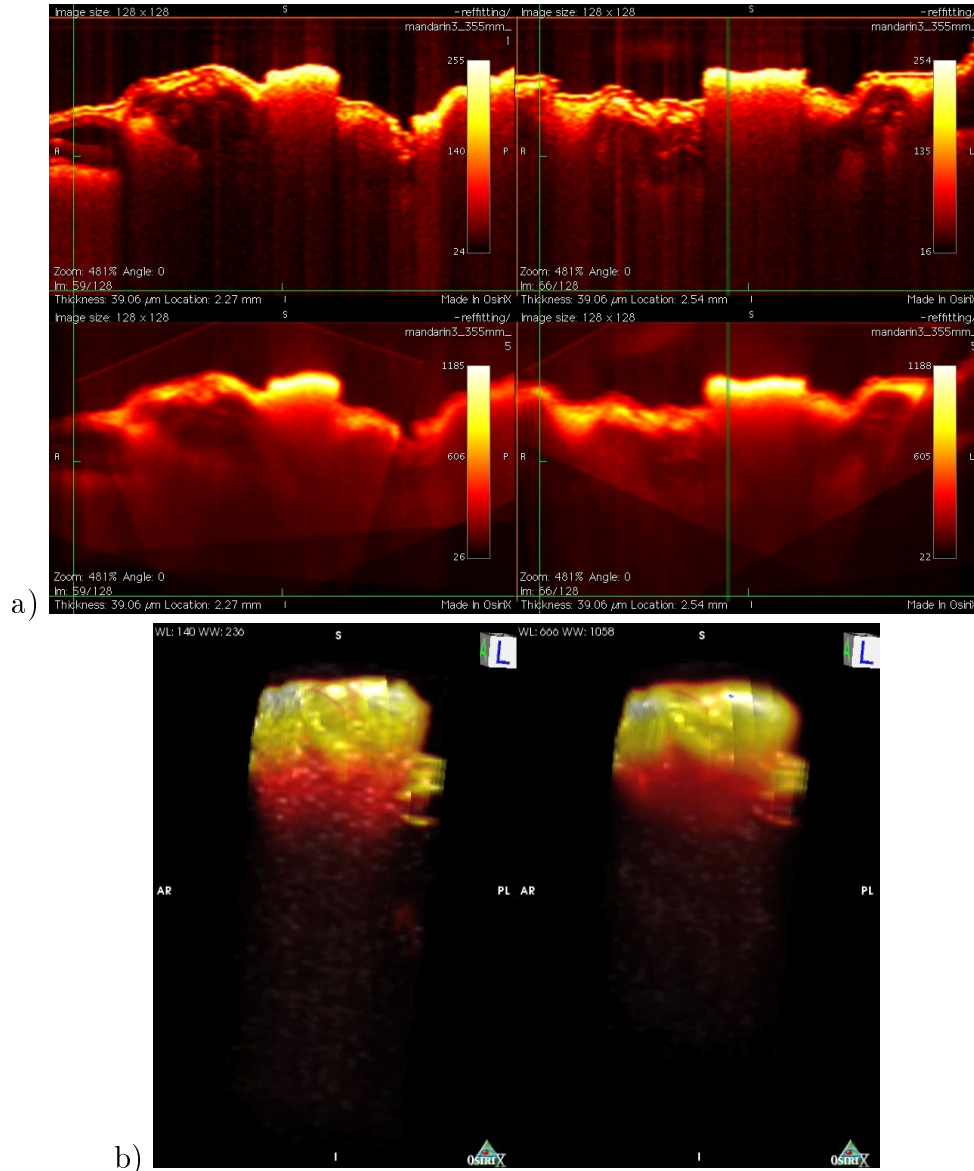


Figure 4.2: a) Top left, shows the reference measurement Y-slice with the shadow from the prestik visible in the middle, to the right is the X-slice of the same. The vertical green line in the X-slice shows where the Y-slice is located. The bottom row shows the same slice as above but with 4 added measurements. b) Shows a 3D image of the shadowed area under the prestik for the reference measurement to the left, and the combined measurement to the right.

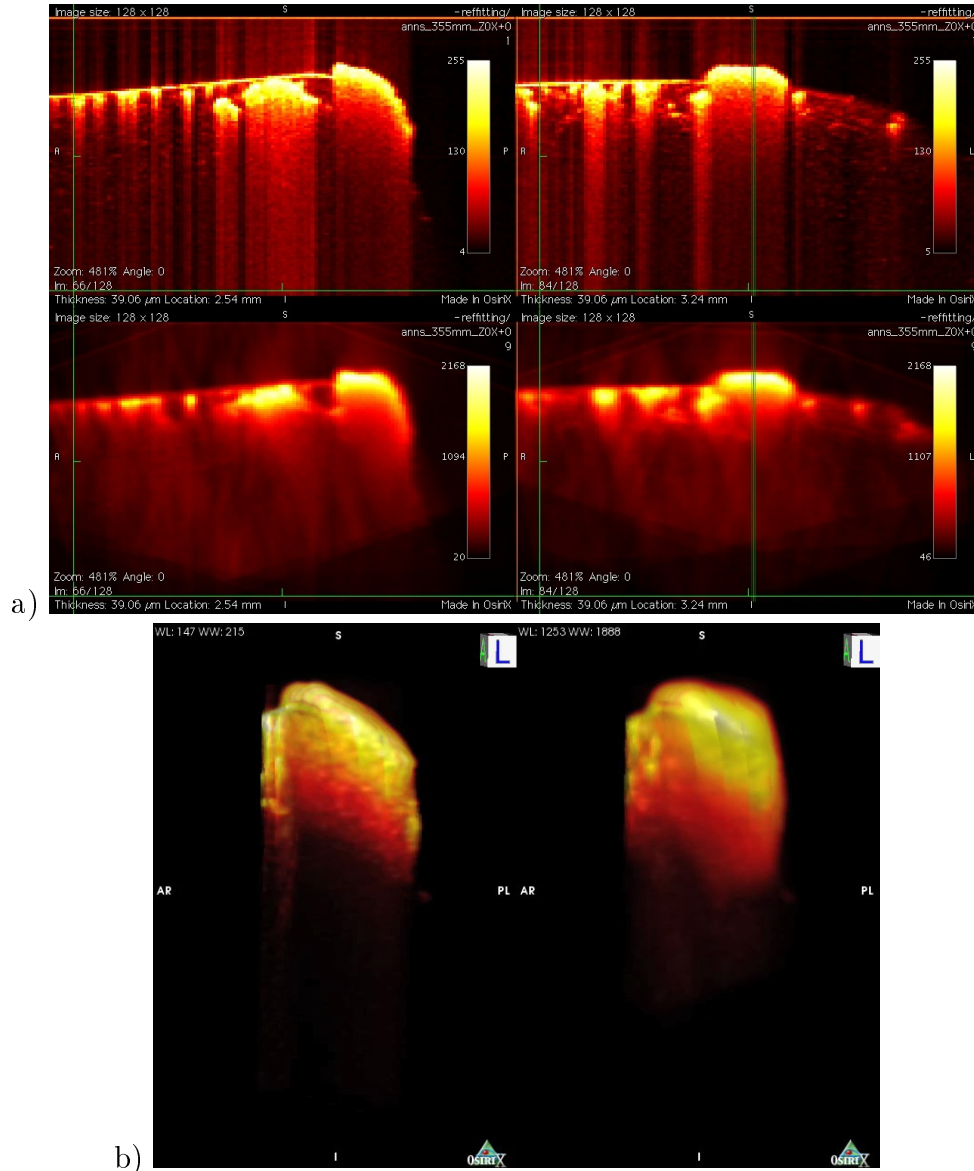


Figure 4.3: a) Top left, shows the reference measurement Y-slice with the shadow from the prestik visible in the middle, to the right is the X-slice of the same. The vertical green line in the X-slice shows where the Y-slice is located. The bottom row shows the same slice as above but with 4 added measurements. b) Shows a 3D image of the shadowed area under the prestik for the reference measurement to the left, and the combined measurement to the right.

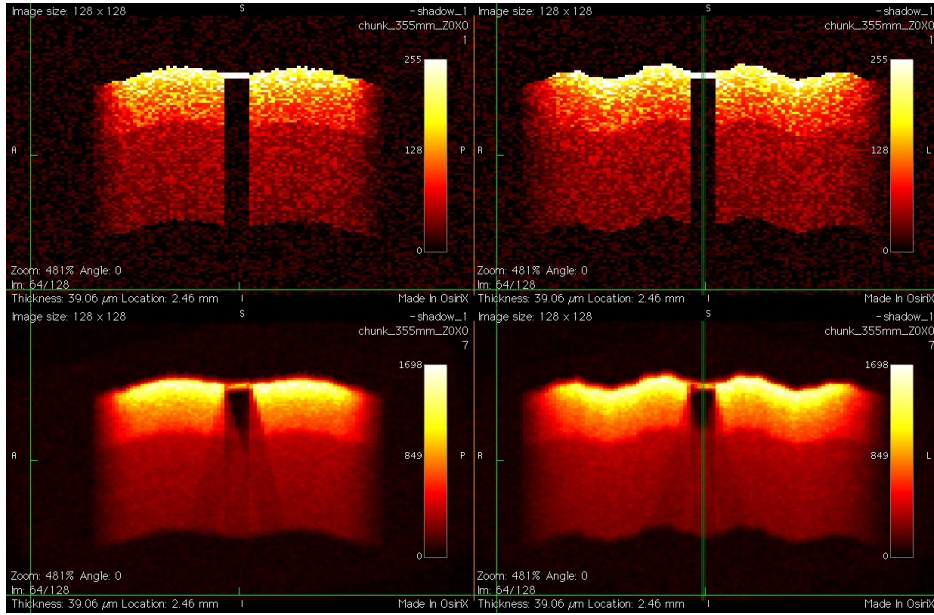


Figure 4.4: Top row to the left shows the reference Y-slice of the test chunk with the 60% shadow visible in the middle, to the right is the X-slice of the same. The vertical green line in the X-slice shows where the Y-slice is located. The bottom row shows the same slice of the 7 automatically aligned and stitched test chunks

4.2 Evaluation of OCT Combine GUI

Aligning the five to nine measurements of the three objects with the two different save methods, six thresholds and four resizing methods together with the nine "measurements" of the test chunk with 5 different shadow strength took almost two days of calculations with the Dell computer. After aligning all measurements, the matrices were exported to DICOM-format which took about half a day resulting in roughly 80 000 images, these were then imported to OsiriX.

4.2.1 Automatic aligning and sensitivity of shadows

A comparison of the reference test chunk and the automatically aligned and stitched test chunks is displayed in Figure 4.4.

The accuracy of aligned test chunks were computed and is displayed in Figure 4.5.

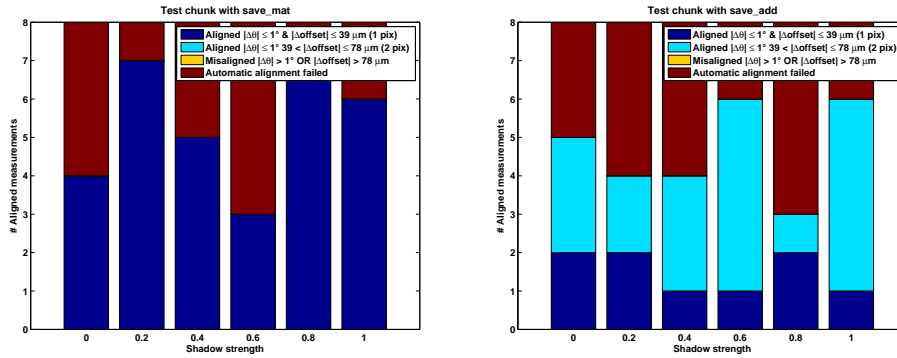


Figure 4.5: The number of automatic alignment of the test chunk depending on the shadow strength with save mode: "save_mat" (left) and "save_add" (right).

4.2.2 Automatic aligning of MAO-OCT measurements

The values of the automatic alignment of the three objects was compared with a manual reference fitting and the result is displayed in Figure 4.6, Figure 4.7 and Figure 4.8.

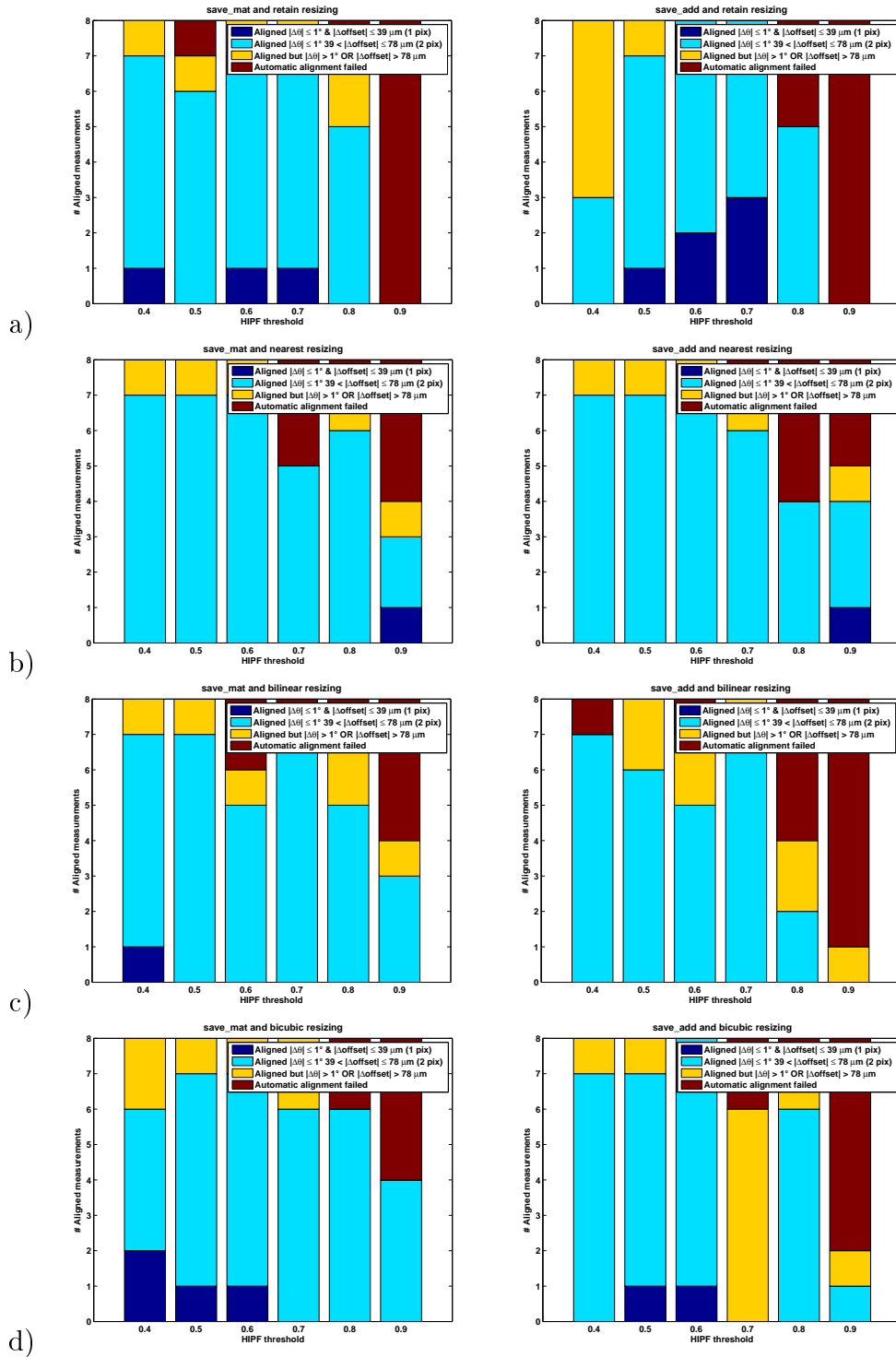


Figure 4.6: The number of automatic fittings of Ann's phantom depending on the HPIF threshold, with save mode: "save_mat" (left) and "save_add" (right). The resizing method is a) retain, b) nearest, c) bilinear and d) bicubic.

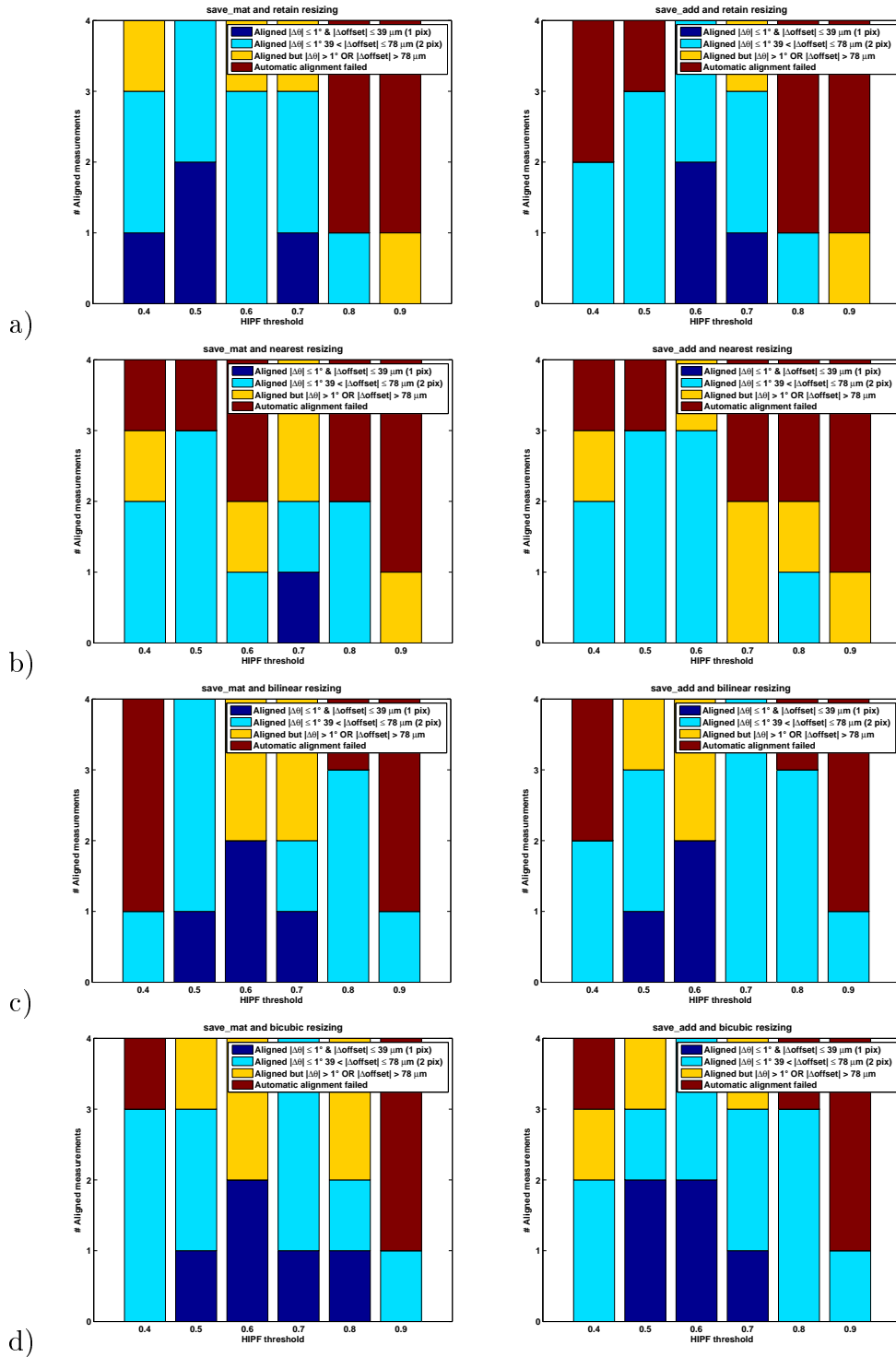


Figure 4.7: The number of automatic fittings of the mandarin depending on the HPIF threshold, with save mode: "save_mat" (left) and "save_add" (right). The resizing method is a) retain, b) nearest, c) bilinear and d) bicubic.

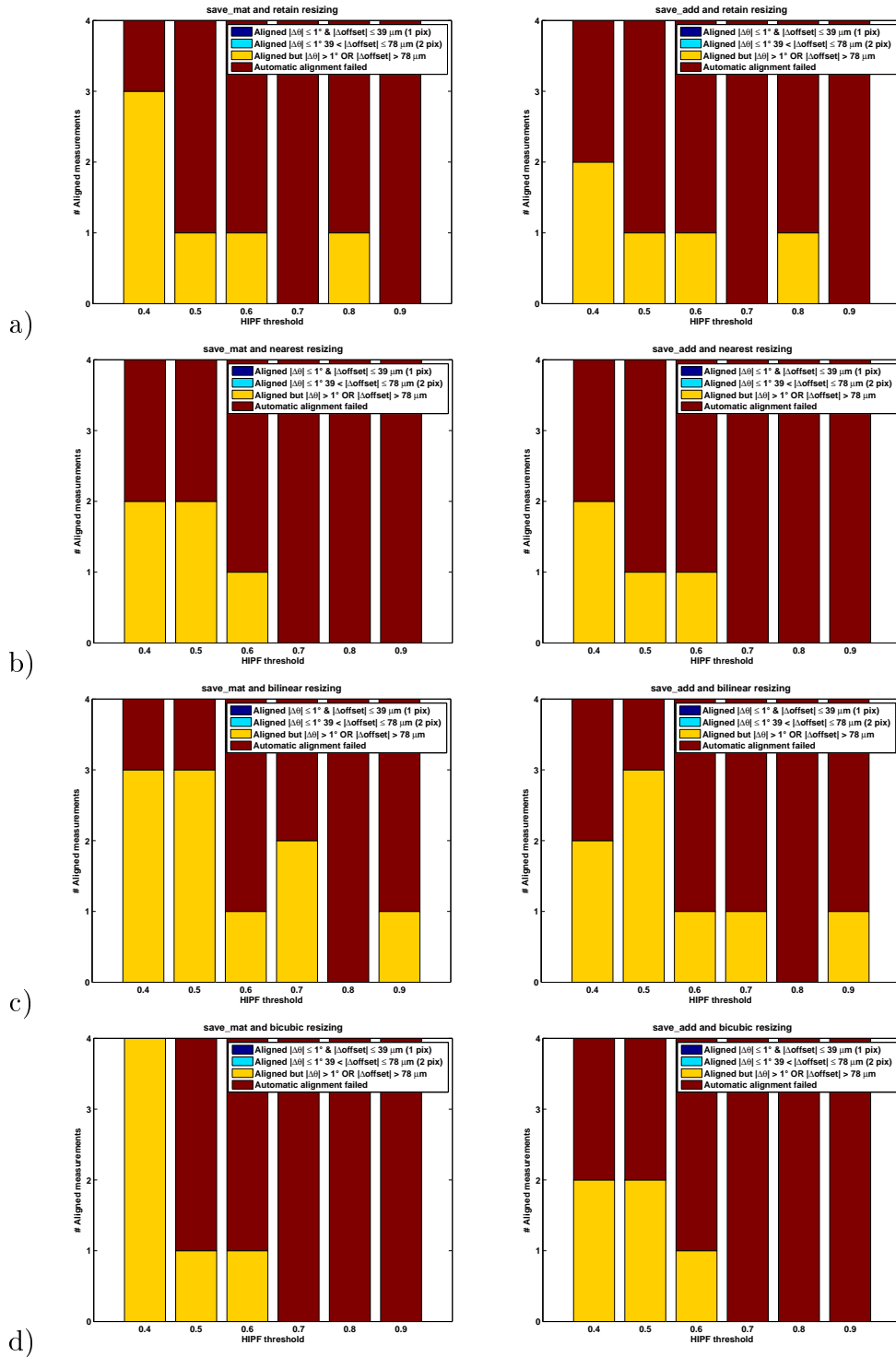


Figure 4.8: The number of automatic fittings of the tape/paper roll depending on the HPIF threshold, with save mode: "save_mat" (left) and "save_add" (right). The resizing method is a) retain, b) nearest, c) bilinear and d) bicubic.

Chapter 5

Discussion

The results in previous chapter shows that it is sometimes possible to display hidden features with MAO-OCT, it also shows that OCT Combine, to some extent, is able to align MAO-OCT measurements automatically. Some of the reasons for the success or failure of the two experiments will be discussed in this chapter.

5.1 Evaluation of MAO-OCT

Even though Figure 4.1 shows that it is possible to display features otherwise shadowed by applying the MAO-OCT technique. Some details are lost due to problems with aligning measurements from different observation angles.

5.1.1 Index of refraction

Differences in refractive index cause objects to look different depending on the observation angle. This phenomena also occurs when watching objects submerged in water, see Figure 5.1. It is therefore impossible to find a perfect alignment of two measurements unless the measurements are taken with the same observation angle, which obviously is not applicable here. The problem causes a blurring effect when adding the measurements together.

5.1.2 Reflections

Strong reflections can raise the whole A-scan making features visible throughout the whole depth of the measurement see Figure 5.2.

When adding MAO-OCT images with reflections together certain features will be more or less hidden behind reflections added from different angles. This results is a decrease in contrast as shown in Figure 5.3



Figure 5.1: A pen in a glass of water illustrating how the index of refraction of different materials can make object look distorted

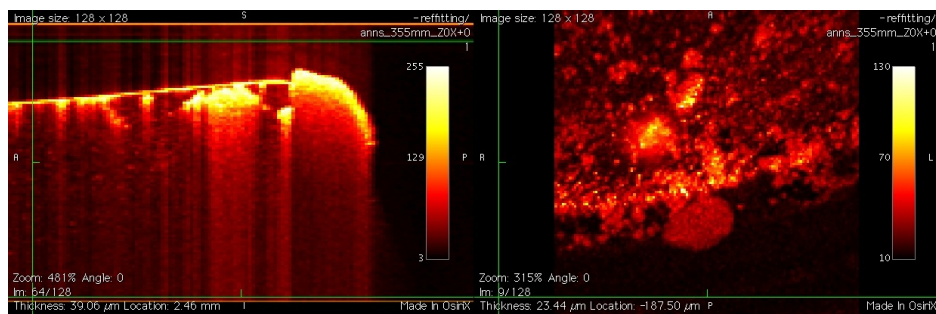


Figure 5.2: To the left a Y-slice of Ann's phantom. The green line indicates the position of the Z-slice to the right. Since there is only air where the Z-slice is taken from, the image should only show noise. This is not the case because of reflections from further down causing a structure to appear.

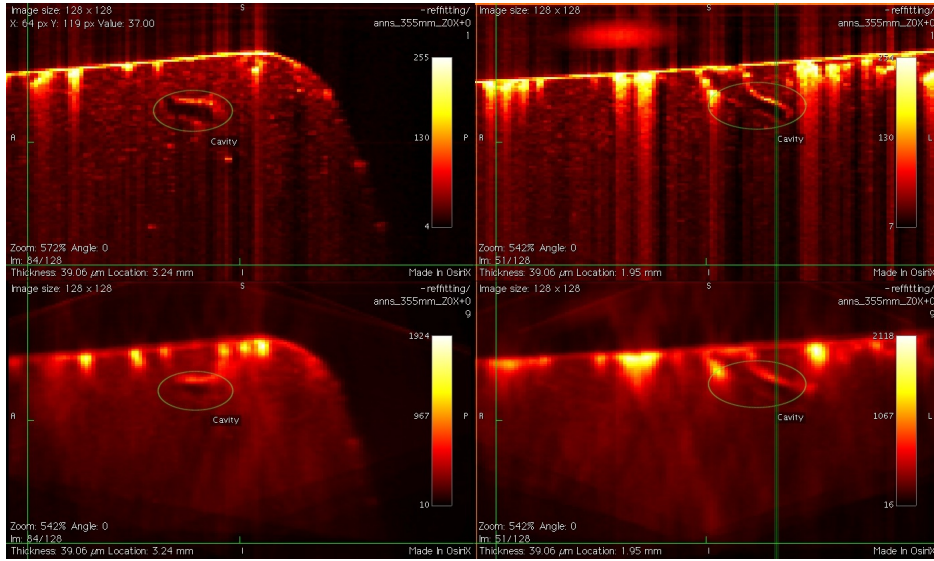


Figure 5.3: Top row displays Y-slice (left) and X-slice (right) of a reference measurement of Ann's phantom. The green line indicates the position of the Y-slice. Bottom row displays the same slices but after adding 8 measurements. The vertical reflections seen in the upper reference images are decreased but the contrast of the cavity is also decreased.

5.2 Automatic aligning capability

5.2.1 Shadow strength

It turns out that the strength of the shadow has a smaller influence on the automatic aligning capability of OCT Combine than one might first expect.

The low influence of the shadow strength can be explained by the HPIF cutting of most of the lower lying layers i.e. taking only a small part of the shadow in to account when aligning the measurements. The small influence it does have on the aligning is noticeable in the `save_add` mode where the misalignment of one measurement will influence the rest, resulting in more misalignments.

5.2.2 Saving method

As mentioned before the misalignment of one measurement will affect the consecutive alignments resulting in fewer "correct" alignments. The general trend in Figure 4.4, Figure 4.6 and Figure 4.7 is that the alignments with the `save_mat` mode are better (more blue) compared with the `save_add` mode.

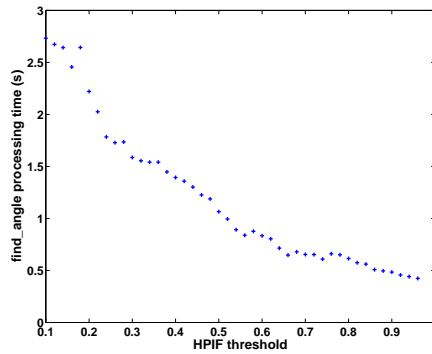


Figure 5.4: The calculation time of `find_angle` as a function of the HPIF threshold.

5.2.3 HPIF threshold

As shown in Figure 5.4, the processing time goes down as the HPIF threshold goes up. One can also see a trend of decreasing number of correct alignments with the higher thresholds in Figure 4.6 to Figure 4.6. A trade off has to be made between processing speed, quality and number of the automatic alignments.

One problem that can be exacerbated by the HPIF is when reflections in two measurements makes different features light up due to different observation angle, see Figure 5.5. When the automatic alignment performs the cross correlation there is a risk that the maximum (the assumed best fit) will not represent the right fit but rather an overlap of the reflections.

5.2.4 Resizing method

The method of resizing seems to have little or no effect on the automatic aligning capability. Therefore it is most useful to use the fastest method retain if the resizing is made only while aligning. If the resized measurement and not the original size is intended to be used after aligning, the bilinear or bicubic method is to be preferred since it incorporates more information from the original measurement than retain.

5.2.5 Other aspects affecting the alignment

One weakness with the golden section search is that it only handles unimodal functions. Here it is assumed that there is only one maximum, which might not always be the case, this implies that a false angle and offset will be found occasionally.

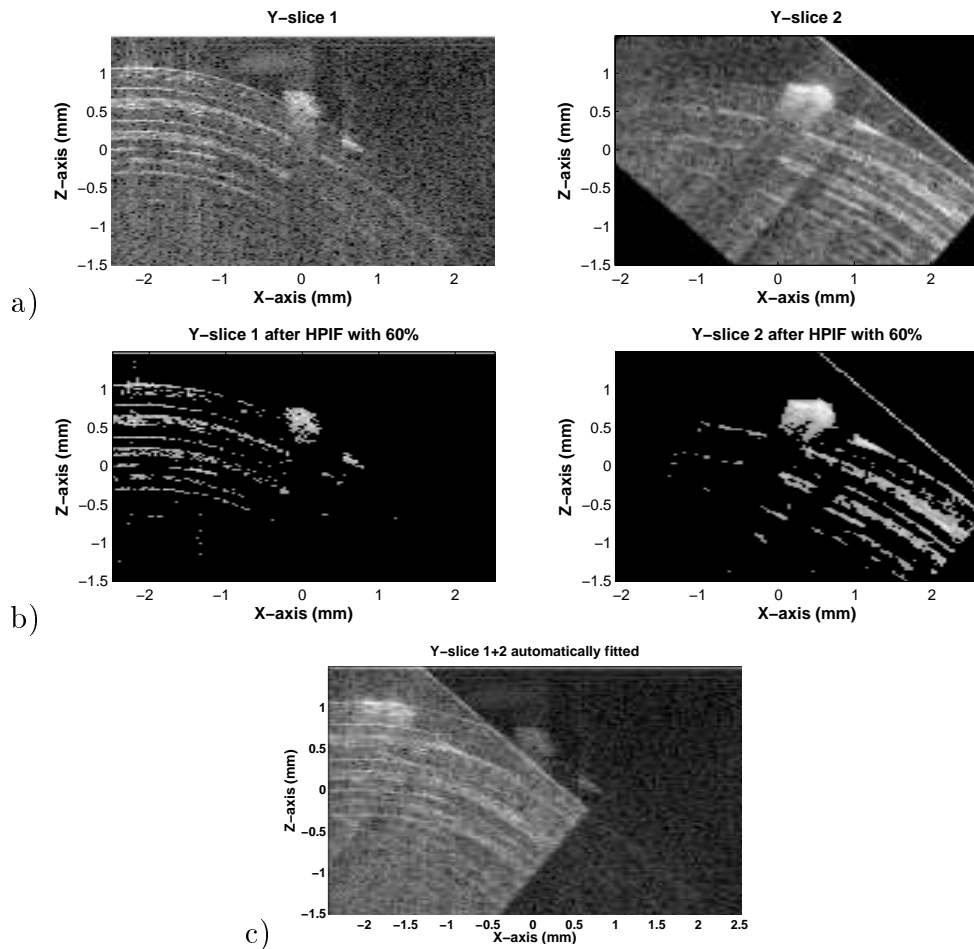


Figure 5.5: a) Y-slices to be aligned b) Y-slices after HPIF at 60% c) shows the incorrect result of the automatic alignment. The prestik in the middle of the Y-slices should preferably be in the same spot.

The choice of ROI turned out to be crucial for the outcome of the automatic aligning. One has to choose a point relatively close to the center of the top layer of the sample. This is to handle miss matching better by having a strong signal to correlate. It is also important that the area to match is neither too random nor uniform but rather with a few distinct features spread out through out the slices.

Since the alignments of the real objects were compared with a subjectively created reference alignment and the influence of the refractive index, the outcome of the tests in subsection 3.2.2 were considered aligned if within the interval $\pm 1^\circ$, see Figure 4.5-Figure 4.8. Outside this interval the alignment started to look incorrect.

Chapter 6

Conclusions and future work

This thesis has shown that it is possible to stitch several measurements together and get the whole picture at once i.e. not having to look at different measurements back and forth. This could have implications in the medical field, for example when examining skin for malignant melanoma. Though the problem with differences in index of refraction and reflections has to be overcome.

It is also shown that the developed software in many cases is capable of finding the alignment of two or more measurement automatically given that the HPIF is not set to high. Another prerequisite for the success of the automatic alignment process is a suitable ROI.

During the course of this project my supervisor and me came up with some ideas that we did not have time to test or implement, but feel should be pursued.

6.1 New measurements

New tests have to be performed on samples with known features in the shadowed volume in order to fully assess the use of MAO-OCT.

6.2 Combining improvements

Now the software works so that measurements are just simply added together. What is proposed for the future is a weighing of the voxels. For example when tilting a measurement the region close to the edge gets padded with zeros, these zeros that carry no information should be weighed with 0.

As seen in subsection 5.1.2 there is a need for reflection reduction. A common way of doing this is by index matching. This can easily be done,

but also proposed is to get a mean value of a few Z-slices in a region of air, like in Figure 5.2, and remove these features through out the whole depth of the sample.

6.3 Aligning improvements

Today a slice of the combination of the reference measurement and the tilted measurement is displayed in OCT combine in order to manually find the offset and tilt. One way to improve the visualization of the overlap is to use colors instead of grayscale. In the combination image give the reference image color green and the second image the color blue and now the areas of good overlap will show up as yellow.


One way to minimize the problem with difference in index of refraction might be to use image registration with a transformation model that allows local deformations, though this might be too labor intensive.

6.4 Future work

OCT Combine could easily be reprogrammed in order to align and save temporal measurements of the same volume. This could allow for monitoring of for example the wound healing process in skin in 4D.

Putting several OCT's together with a 90° or some other known angle to each other and do simultaneous measurements of the "exact" same volume might "shed some light" on the optical properties of it such as index of refraction.

Bibliography

- [1] Digital imaging and communications in medicine (dicom). multi-part document, 2008. 
- [2] Mark E. Brezinski Bin Liu. Theoretical and practical considerations on detection performance of time domain, fourier domain, and swept source optical coherence tomography. *Journal of Biomedical Optics*, 12(4):044007–1–12, July/August 2007.
- [3] Mark E Brezinski. *Optical Coherence Tomography: Principles and Applications*. Academic Press, 30 Corporate Drive, Suite 400, Burlington, MA 01803, USA, 1 edition, 2006.
- [4] M.E. Brezinski and J.G. Fujimoto. Optical coherence tomography: high-resolution imaging in nontransparent tissue. *Selected Topics in Quantum Electronics, IEEE Journal of*, 5(4):1185–1192, Jul/Aug 1999.
- [5] A E Desjardins, B J Vakoc, A Bilenca, G J Tearney, and B E Bouma. Estimation of the scattering coefficients of turbid media using angle-resolved optical frequency-domain imaging. *Opt Lett*, 32(11):1560–1562, 2007.
- [6] Gerd Eriksson. *Numeriska Algoritmer med MATLAB*. NADA,KTH, KTH CSC, Lindstedtsvägen 3, 100 44 Stockholm, June 2002.
- [7] AF Fercher, W Drexler, CK Hitzenberger, and T Lasser. Optical coherence tomography - principles and applications. 66:239–303, 2003. Reports On Progress In Physics.
- [8] Lida P. Hariri, Alexandre R. Tumlinson, David G. Besselsen, Urs Utzinger, Eugene W. Gerner, and Jennifer K. Barton. Endoscopic optical coherence tomography and laser-induced fluorescence spectroscopy in a murine colon cancer model. *Lasers in Surgery and Medicine*, 38:305–313, 2006.

- [9] Ann Johansson. *Spectroscopic Techniques for Photodynamic Therapy Dosimetry*. PhD thesis, Lund University, Division of Atomic Physics, Department of Physics, Faculty of Engineering, LTH, Lund University, P.O. Box 118, SE-221 00 Lund, Sweden, 2007.
- [10] Alexander I Kholodnykh, Irina Y Petrova, Kirill V Larin, Massoud Motamedi, and Rinat O Esenaliev. Precision of measurement of tissue optical properties with optical coherence tomography. *Appl Opt*, 42(16):3027–3037, 2003.
- [11] Marcelo Soto Thompson. *Photodynamic Therapy utilizing Interstitial Light Delivery Combined with Spectroscopic Methods*. PhD thesis, Lund Institute of Technology, Division of Atomic Physics, Department of Physics, Faculty of Engineering, LTH, Lund University, P.O. Box 118, SE-221 00 Lund, Sweden, October 2004.
- [12] Thorlabs, Thorlabs, Inc. 435 Route 206 Newton, NJ 07860 USA. *Swept Source OCT System Operating Manual*, 14126-d02 rev b 09/06/07 edition.
- [13] Alexandre R. Tumlinson, Lida P. Hariri, Urs Utzinger, and Jennifer K. Barton. Miniature endoscope for simultaneous optical coherence tomography and laser-induced fluorescence measurement. *Applied Optics*, 43(1):113–121, January 2004.
- [14] User:PAR, Charles Matthews, Phil Boswel, Ligulembot, Casey Abell, Finell, SmackBot, Mark Walter, David Eppstein, Avalcarce, and Giftlite. Golden section search. Wikimedia Foundation, Inc., June 2008.
- [15] User:Pumpkinegan. Oct b-scan setup.gif. Wikimedia Foundation, Inc., March 2006. This work is licensed under the Creative Commons Attribution-ShareAlike 2.5 License.

Appendix A

Getting started with OCT Combine

Getting started with OCT Combine v1.3

This guide will take you through the basic steps in using OCT Combine to combine two or more measurements.

Definitions

Orientation: Here a right hand coordinate system is used and the orientation of the axes relative to the laser are shown in Figure 1 below:

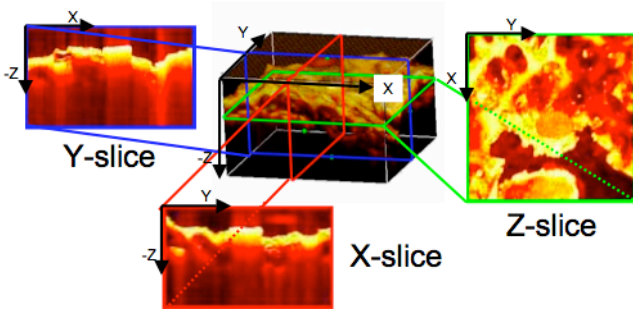


Figure 1 Slice orientation (green=Z-slice, red=X-slice and blue=Y-slice)

Rotation: The rotation θ_z means the right hand rotation around the Z-axis.

Loading files

When you start the software you will see a window like in Figure 2:

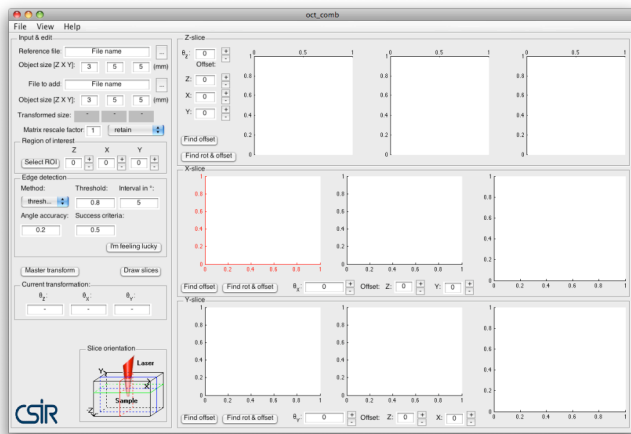


Figure 2 Screenshot of oct_comb

1. Specify the “Object size [Z X Y]” in millimeters for the reference measurement and the measurement you want to combine. Also specify if you want to use a “Rescale matrix factor” i.e. display and perform all calculations with a scaled down matrix. A factor of 0.5 reduces the size of all dimensions for the input files to $\frac{1}{2}$ (matrices

larger than [256 256 256] produce quite long calculation times on a MacBook 2 Ghz Intel Core Duo with 2 GB 677 MHz RAM).

2. Go to menu File>Load Files and follow the instructions. When asked to specify Region Of Interest (ROI) click on the displayed picture. First you choose the depth i.e. Z-axis, then a slice at the specified depth will be displayed and you get to choose the value along X/Y-axis to be displayed.
3. After some loading (and resizing of matrices, if chosen) a slice at each axis will be displayed in the panels to the right.

Finding the rotation and offset

Now you can start rotating and nudging the second measurement in order to align the measurements by changing the values in the “Offset:” fields.

Note that rotating the images in the “Z/X/Y-slice” panels does not rotate the whole 3D-matrix, only the current slice. To rotate the 3D-matrix specify the change of angle in the θ -field ($\theta_z: 0$) for the Z/X/Y-axis respectively then push the button **Master transform**. Now a rotation of the input matrix will be performed in the along the axes in the following order Z, X then Y.

Note the offsets displayed in the Z-slice panel specify which slices are shown in the other two panels. The offsets in the X/Y-slice panel specifies the offset if the current image (after rotation).

Automatic search for rotation and offset

If the measurements are not too dissimilar you can try to find the best fit automatically with a golden section search by pushing the **Find rot & offset**-button. First you need to adjust the following:

1. In the panel “Edge detection” specify the method to use (default is “threshold” i.e. remove all the pixels below the threshold).
2. Specify the threshold value in the “Threshold”-box, (for method “threshold” choose an absolute value $1 < t < 255$ or a fraction of the maximum image value $0 < t < 1$. See “Matlab Help” [1] to specify threshold for the other methods).

- The golden section search algorithm will stop when the difference between two calculations are smaller than the specified “Angle accuracy”.
- The golden section search algorithm will search for the rotation around the current specified angle +/- the value in “interval in $^{\circ}$ ”.

You can also try your luck with the **Im feeling lucky** button, which performs a series of golden section searches and “Master transformations” in order to find the best rotation and offset combination, a message in the command window will notify you of success/failure.

Save/export and add new measurement

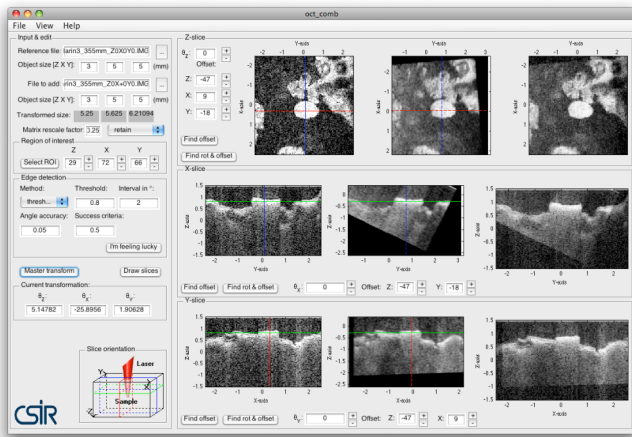


Figure 3 Aligned measurement ready for export

First make sure that the alignment look good when the X/Y/Z-offset are the same in all the panels. Then you are done with the aligning you can do either of the following:

File>Save combination to .mat: In which the two current measurements are added together with the rotation specified in “Current transformation” and saved in a .mat-file. The matrix is named OCT and the resolution dimension of the pixels are stored in the variable T (as [row column depth] (mm/pixel))

File>Save and add new file: In which the two current measurements are added together with the rotation specified in “Current transformation”. Then you are asked to locate the next measurement to add.

File>Save current session: In which all the settings are saved to a .mat-file. This file can then be loaded later.

File>Export>to DICOM: In which the two current measurements are added together with the rotation specified in “Current transformation” and saved as a series of DICOM-images. The images will be all the consecutive Y-slices.

Requirements

In order to use this software the Image Toolbox must be present.

References

- The Mathworks Matlab & Image Toolbox, Software available from: <http://www.mathworks.com>

Appendix B

OCT Combine flowchart

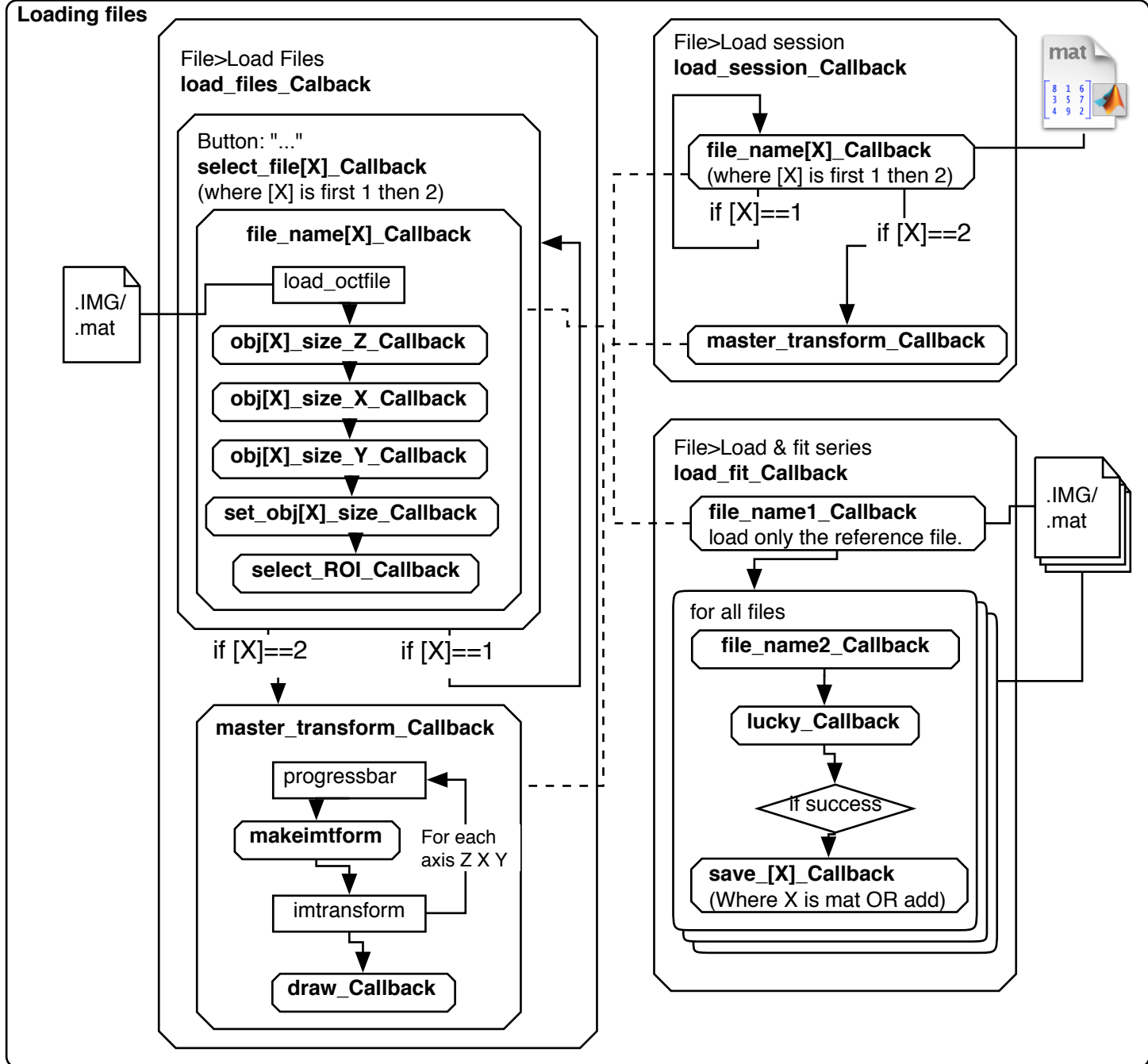
This flowchart explains the basic flow of the functions in OCT Combine 1.3. For more exact explanation of the workings of the functions peels refer to the source code.

Convention:
Dashed line "-" means same function

["Button" or Menu>submenu]
internal function name
(comment)
functions used

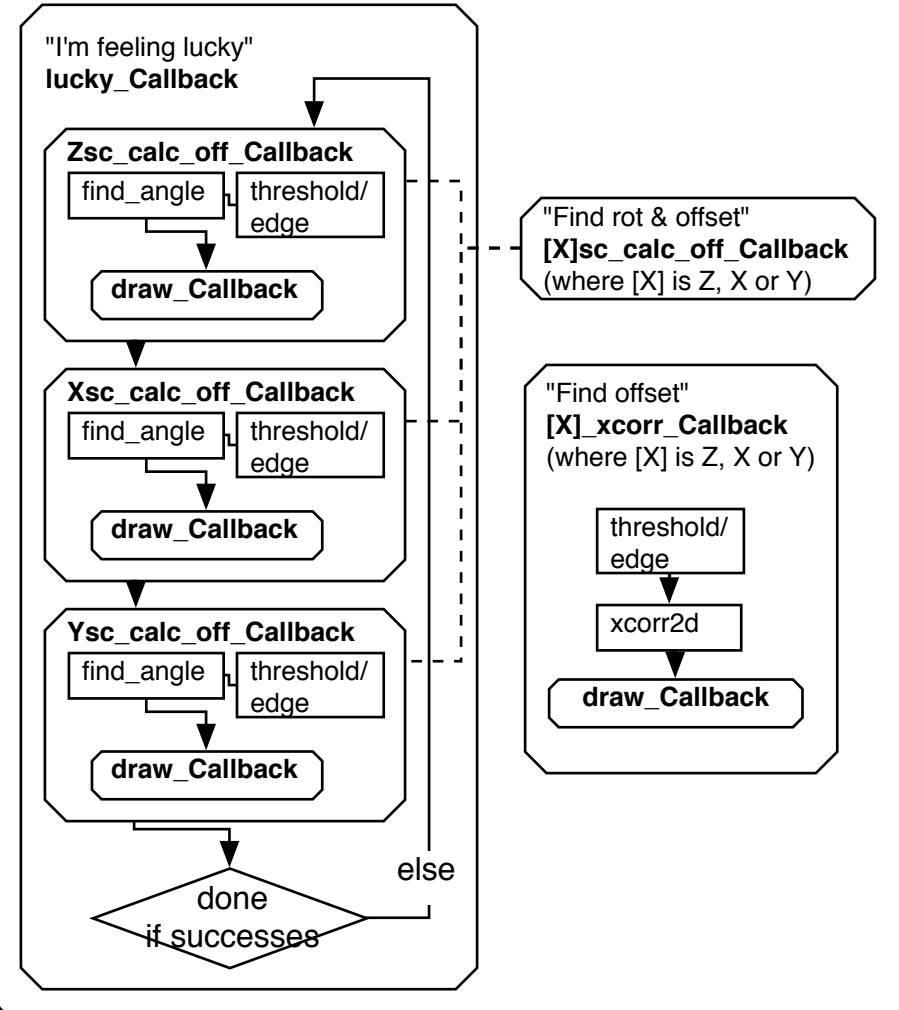
external function [optional]

iterative area
file-stack
file



Calculating rotation and offset

(Success criteria, angle "diff"<0.5, see source code for more info)



Saving and exporting

